Acta Cryst. (1973). A**29**, 489

Studies of the Lattice Parameters and Domains in the Phase Transitions of $NaNbO_3$

BY A. M. GLAZER AND H. D. MEGAW

Cavendish Laboratory, Cambridge, England

(*Received* 9 *February* 1973; *accepted* 22 *March* 1973)

The lattice parameters of $NaNbO_3$ have been measured to a precision between 1 part in 10^5 and 1 part in 10^4 at temperatures up to 800 °C. Six distinct phases are found: P (room temperature to 373 °C), R(373–480 °C), S(480–520 °C), T_1(520–575 °C), T_2(575–641 °C), cubic (> 641 °C). Coexistence of phases S and T_1 between 520 and 535 °C has been found, together with twinning effects, and a possible explanation for this is given.

1. Introduction

Sodium niobate, $NaNbO_3$, a member of the perovskite family, has been the subject of several independent crystallographic studies: for example, Wood (1951), Solov'ev, Venevtsev & Zhdanov (1961), Izmailzade (1963), Tennery (1965), Lefkowitz, Łukaszewicz & Megaw (1966). A survey of the earlier work was given by the last-named authors (referred to hereafter as LLM), who described a number of new phases.

The structural differences between any of the phases are very slight, amounting to small distortions of the cubic aristotype, and therefore very accurate techniques are needed to study them. Though powder methods make it easy to achieve accurate and sensitive temperature control of the specimen, and to measure lattice spacings accurately, they have inherent disadvantages: they do not show which spacings are associated with which direction in reciprocal space, nor, when more than one phase is present, can the lines attributable to each be easily sorted out; moreover, weak lines are easily lost in the background. Single-crystal methods correlate the spacings with particular directions in space; if the crystal is twinned, or has two phases coexisting at the same temperature, the reflexions due to each kind of domain can be distinguished. Moreover, at a transition it is, in principle, possible to see how the orientation of the new phase is related to that of the old. One disadvantage of the method is that only two of the three spacings of each domain are recorded from a single setting of the crystal; this is partly overcome by the fact that differently oriented domains, present on the same or successive runs, may provide complementary information. Other disadvantages are the difficulty of good temperature control, and the possibility of errors in spacing measurement due to mis-setting of the crystal – mis-setting which is liable to occur when the crystal is heated or cooled through transitions too rapidly or in an uncontrolled way. Both these difficulties affected the work of LLM. Though they were partly obviated by giving more weight to differences of spacings measured on the same or successive photographs, and differences of temperatures between photographs of the same run, than to absolute values, the precision thus achieved in the construction of the lattice-parameter plot could not be high. The work of LLM must therefore be regarded as a pilot study.

For the present work, a new furnace was devised, with specially designed controls (§ 2.1). Greater precision of lattice parameter measurements was achieved by using a double-radius film holder and introducing an extrapolation procedure for the measured spacings (§ 2.2). The smoothness of the temperature control not only effectively eliminated spontaneous mis-setting of the crystal, but also made it possible to follow the identity of particular domains through their various transitions (§ 4).

It was satisfying to find that the main features of the pilot study were reproduced in the newer, more precise, work reported here. Some of the older detail was, however, too close to its limits of resolution to be very reliable, and here the new work has given clearer information.

2. Experimental work

Two small crystals ($\simeq 0{\cdot}2 \times 0{\cdot}2 \times 0{\cdot}2$ mm) were selected from separate batches, kindly given to us by R. C. Miller of Bell Telephone Laboratories, and were used in all the work reported here. Crystal No. 1 was used for initial measurements of lattice parameters (run 1) and crystal No. 2 for subsequent measurements (run 2). Two further runs with crystal No. 2 were used in an additional study of domain formation and the direct comparison of lattice-parameter changes.

There are three major aspects of the experimental work to consider, namely temperature control, lattice-parameter measurements, and twinning and domain formation.

2.1 *Temperature control*

A full description of the temperature-controlling system and furnace is published elsewhere (Bett & Glazer, 1972).

The small furnace, capable of being mounted on a Weissenberg goniometer head, consisted of a heating coil, placed above and below the crystal specimen, both

coils being held within pyrophyllite cylinders. The gap between the cylinders gave an estimated angle of about 300° around the crystal for the emergence of diffracted beams. The crystal specimen was mounted on the tip of a chromel/alumel thermocouple (0·0076 in diameter wires) with alumina cement. The signal from the thermocouple was fed to a specially designed three-term controller (designed and built in the Electronics Section at the Cavendish Laboratory). The temperature could be raised and lowered smoothly at rates between 2·5 °C/hour and 1·6 °C/sec. In practice, we found that temperatures up to 900 °C could be held steady to within $\pm\frac{1}{4}$ °C. Absolute measurements of the temperature, however, were unreliable, since the thermocouple wires were subject to deterioration with time. This difficulty was overcome as follows. For the first lattice-parameter run, the thermocouple voltage was converted to 'initial temperature' by the use of the standard calibration curve (Natl. Bur. Stand. 508), which is not far from linear. The 'initial temperatures' of the two main transitions were then plotted against the values of 373 and 641 °C recorded by Denoyer, Comès & Lambert (1971) (referred to as DCL hereafter) using DTA techniques, and a smooth correction curve was drawn through these points, marked with crosses in Fig. 1, and room temperature. Points representing the other transitions, for which temperatures were also measured by DCL, lay close to this curve.

For the second lattice-parameter run, the same thermocouple was used, supplemented by a Pt/Pt–Rh(13%) thermocouple mounted above and close to the specimen. If the lattice spacings were plotted against temperatures read from the latter thermocouple, they lay very close to those from the first run using the correction curve mentioned above. If the chromel/alumel temperatures, corrected as for the first run, had been used for the second run, agreement would not have been satisfactory. This is easily explained by the well known aging of chromel/alumel. Our procedure in using the Pt/Pt–Rh thermocouple amounted to the same thing as constructing a new correction curve.

With our apparatus, it was possible to conduct a complete run over two or three months continuously, without lowering to room temperature. This was particularly important, since $NaNbO_3$ single crystals tended to twin increasingly, or even break up, with temperature cycling. During the second run, the temperature was raised at a rate of $\frac{3}{4}$ °C per minute between sets of X-ray photographs. This slow increase in temperature meant that mis-setting of the specimen was reduced to a minimum. In any case, if resetting had become necessary, our apparatus would have permitted this even at the highest temperatures.

2.2 *Lattice-parameter measurements*

A back-reflexion, double-radius film holder (R= 57·3 mm, Stoe & Cie.) was used throughout. On each film, several 40° oscillation photographs of the zero layer were taken, either at different azimuthal angles or with successive increments of temperature. Unfiltered Cu radiation was used, giving Cu $K\beta$ in addition to the usual Cu $K\alpha$ doublet; impurities in the target also gave rise to W L lines, which, though weak, were useful in certain cases. The positions of the reflexions were measured with a travelling microscope to ±0·01 mm.

Several techniques were initially considered for extracting the maximum precision from the data. We finally decided to use Cohen's (1935) analytical extrapolation procedure. The possible sources of error are eccentricity of the specimen and of the oscillation axis, absorption, and angular mis-setting of the crystal. Of these, angular mis-setting, though potentially serious, has received least attention in the literature. Fortunately, in neither run did our crystals become sufficiently mis-set to affect the final parameters, as could be seen by the way the spots on the zero layer lay nearly always in a straight line. For the other errors, we assumed that the extrapolation formulae as given by Buerger (1966), though designed for powders, would be satisfactory for our purposes. In practice, only the eccentricity correction proved to be important.

In general, at least 8 reflexions were used for each extrapolation, with $\theta > 60°$; for example at 607 °C they were

330 (Cu $K\alpha_1$, Cu $K\alpha_2$)
420 (Cu $K\alpha_1$, Cu $K\alpha_2$)
500 (Cu $K\alpha_1$, Cu $K\alpha_2$)
510 (Cu $K\alpha_1$, W $L\alpha_1$)
050 (Cu $K\alpha_1$, Cu $K\alpha_2$)
150 (Cu $K\beta$, W $L\alpha_1$, Cu $K\alpha_1$)
250 (Cu $K\beta$).

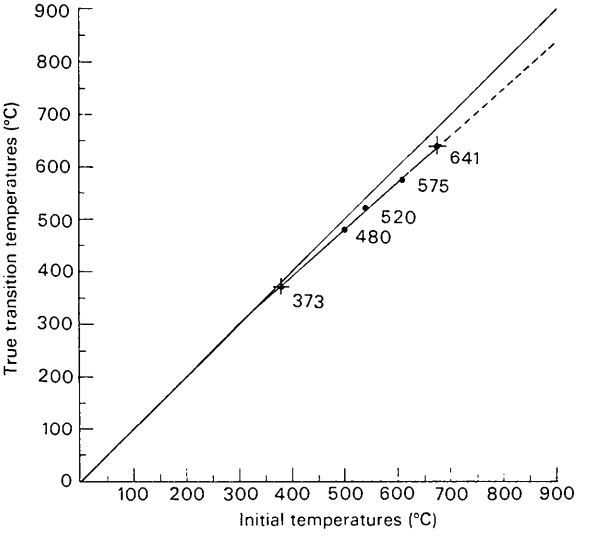

Fig. 1. Correction curve for chromel/alumel thermocouple (run 1). The true transition temperatures were those measured by Denoyer, Comès & Lambert (1971): 'initial temperatures' refer to those obtained by direct conversion of our thermal e.m.f.'s according to the standard curve.

Relative weights were assigned to the measurements according to the intensities I and the widths Δ of the spots; if the error in the estimated positions is assumed to be proportional to Δ and inversely proportional to I, the weights are

$$w \propto I^2/\Delta^2.$$

Although an estimated standard deviation was calculated for each extrapolated lattice parameter, the most reliable estimate of the overall accuracy in lattice parameter comes, we feel, from the scatter in the plot against temperature. This was estimated to be about 1 part in 10^5 at the lowest temperatures and about 1 part in 10^4 at the highest temperatures. The individually estimated standard deviations were always less than this, too small to be shown in the plot given here (Fig. 2) without confusion.

2.3 *Twinning and domain behaviour*

The shapes and splittings of the spots gave a great deal of information about the twin domains in $NaNbO_3$. Additional evidence of these domains was obtained by taking Weissenberg photographs at intervals during the runs, and also by taking several oscillation photographs on the same film as the temperature was either raised or lowered at a rate of $\frac{3}{4}$°C/min (runs 3 and 4). During this latter type of experiment, the film holder was displaced laterally by 1 mm every 5 minutes (Glazer, 1972*a*). The effect of this was to provide a continuous record of the spot behaviour with temperature, a technique similar to that of Milledge (1966). Since the reflexions lie on the equatorial line of the oscillation photograph, at a distance from the back-reflexion position which is a simple function of their spacings, and the translations corresponding to temperature intervals are perpendicular to the equatorial line, such a photograph printed with the equatorial line vertical on the page actually reproduces part of a graph similar to Fig. 2. In Fig. 3 we show a composite made from several such photographs covering the entire temperature range.

3. Discussion of the lattice-parameter study

Fig. 2(*a*) shows the plot of pseudocubic subcell parameters a_p, b_p and c_p *versus* temperature and Fig. 2(*b*) that of the angle β in phase P. The smooth curves were drawn from least-squares fitting of the data to polynomials of degree 1, 2 or 3.

In Fig. 2(*a*) we can distinguish six separate phases and these are summarized in Table 1 [actually, an additional low-temperature phase, N (Darlington, 1971), has been included in the Table for the sake of completeness]. As mentioned in § 1, Fig. 2 is similar to the earlier plot of LLM, but differs in detail in the region between 373 and 600 °C.

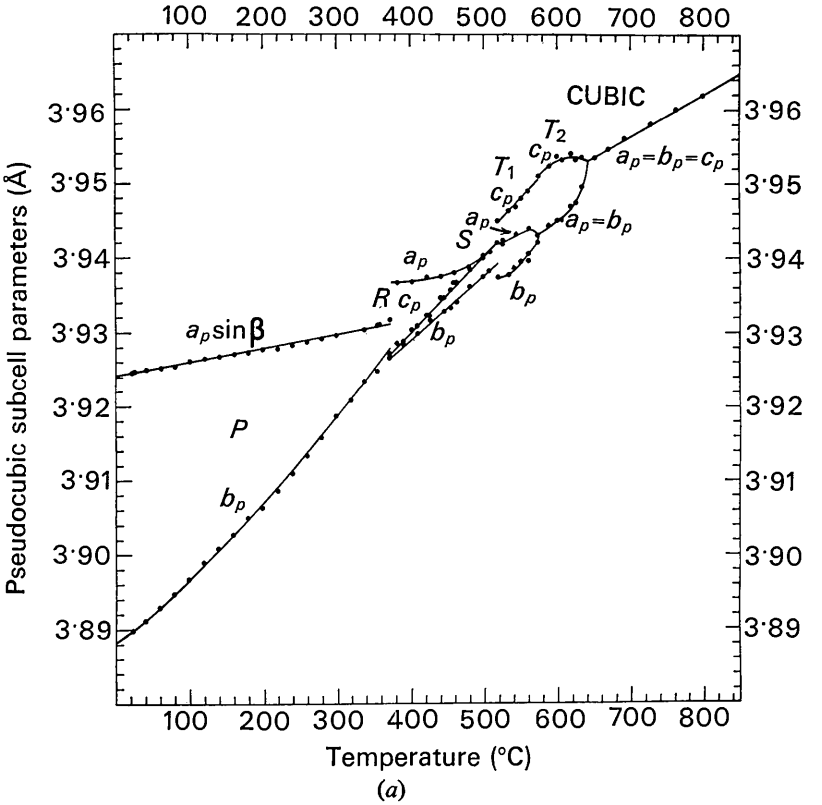

(*a*)

Fig. 2. Plot of lattice parameters as a function of temperature, (*a*) pseudocubic subcell edge lengths.

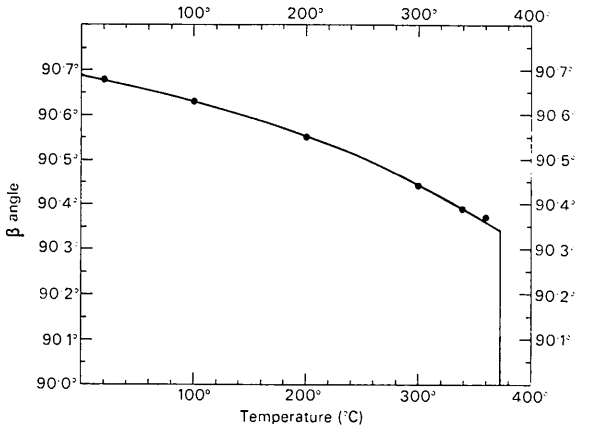

(*b*)

Fig. 2 (*cont.*) (*b*) β-angle in phase *P*.

At all temperatures above 373 °C, the earlier work indicated that the pseudocubic axes of reference were all orthogonal, and this conclusion is supported by the present work.

The three spacings in phase *S* are so closely alike that LLM could not distinguish them unambiguously. In this study we see that the onset of the phase is characterized by a rapid but apparently continuous change of slope of the temperature variation of a_p. The convergence of the two larger spacings near 500 °C is probably accidental and does not imply tetragonal symmetry.

From this work, we could not have said that *R* and *S* were necessarily separate phases; the evidence for this comes from other sources (for example, DCL). All the other transitions on the diagram show up clearly, being marked by discontinuous changes in subcell parameters or their slopes. The phase *W* shown in the photographs of LLM is no longer apparent as a distinct phase and in fact can be explained in terms of the coexistence of phases *S* and T_1 (§ 4).

Phases T_1 and T_2 are recognizably similar to those reported by LLM, and the discontinuity tentatively suggested by them at the T_1–T_2 transition is now confirmed for c_p. This was apparent not only from the calculation of lattice parameters, but also by visual inspection of the continuous-recording photographs (not easily seen in the reproduction). These photographs also showed the convergence of the two lower spacings a_p and b_p in T_1 to the lower spacing in T_2, and that of c_p and a_p in T_2 to a single spacing in the cubic phase, as indicated by the arrows in Fig. 3(*a*). These facts have been used as evidence in our detailed study of the T_2–T_1 transition (Ahtee, Glazer & Megaw, 1972).

4. Domain behaviour

From observations of the splitting of reflexions on photographs taken during the four runs it was possible to identify particular domains. Because of the high absorption of the incident Cu $K\alpha$ radiation by the crystals, our photographs only depict the surface domains. Much of this work was done with the photographs shown in Figs. 3 and 5.

With very slow rates of heating and cooling (less than 1 °C/min) we observed that the relative orientations of the crystal above and below each transition tended to be the same in all the runs. We therefore chose to name the lattice parameters so that a_p, b_p and

Table 1. *The phases of* $NaNbO_3$

Temperature	Phase	Symmetry	Pseudocubic cell	Tilt system	Cation displacement	Reference
	N	Rhombohedral	$2a_p \times 2b_p \times 2c_p, a_p = b_p = c_p$	$a^-a^-a^-$	3 corner [111]	Darlington (1971)
~50 °C						
	P	Orthorhombic (in rhombic orientation)	$2a_p \times 4b_p \times 2c_p, a_p = c_p > b_p$	$a^-b^+a^-$; $a^-b^-a^-$*	2 corner [10$\bar{1}$]	Sakowski-Cowley, Łukaszewicz & Megaw (1969)
373						
	R	Orthorhombic (in parallel orientation)	$2a_p \times 6b_p \times 2c_p, a_p > c_p > b_p$	$a^-b^+c^+$; $a^-b^0c^+$*	1 corner [100]	Sakowski-Cowley (1967)
480						
	S	Orthorhombic (in parallel orientation)	$2a_p \times 2b_p \times 2c_p, a_p > c_p > b_p$	$a^-b^+c^+$	–	Ahtee, Glazer & Megaw (1972)
520						
	T_1	Orthorhombic (in parallel orientation)	$2a_p \times 2b_p \times 2c_p, c_p > a_p > b_p$	$a^-b^0c^+$	–	Ahtee, Glazer & Megaw (1972)
575						
	T_2	Tetragonal	$2a_p \times 2b_p \times c_p, c_p > a_p = b_p$	$a^0a^0c^+$	–	Glazer & Megaw (1972)
641						
	Cubic	Cubic	$a_p \times b_p \times c_p, a_p = b_p = c_p$	$a^0a^0a^0$	–	–

* Phase *P* and *R* have complicated tilt systems. Phase *P* has pairs of $a^-b^+a^-$ layers alternating with pairs of $a^-b^-a^-$ layers. Phase *R* has pairs of $a^-b^+c^+$ layers alternating with single $a^-b^0c^+$ layers.

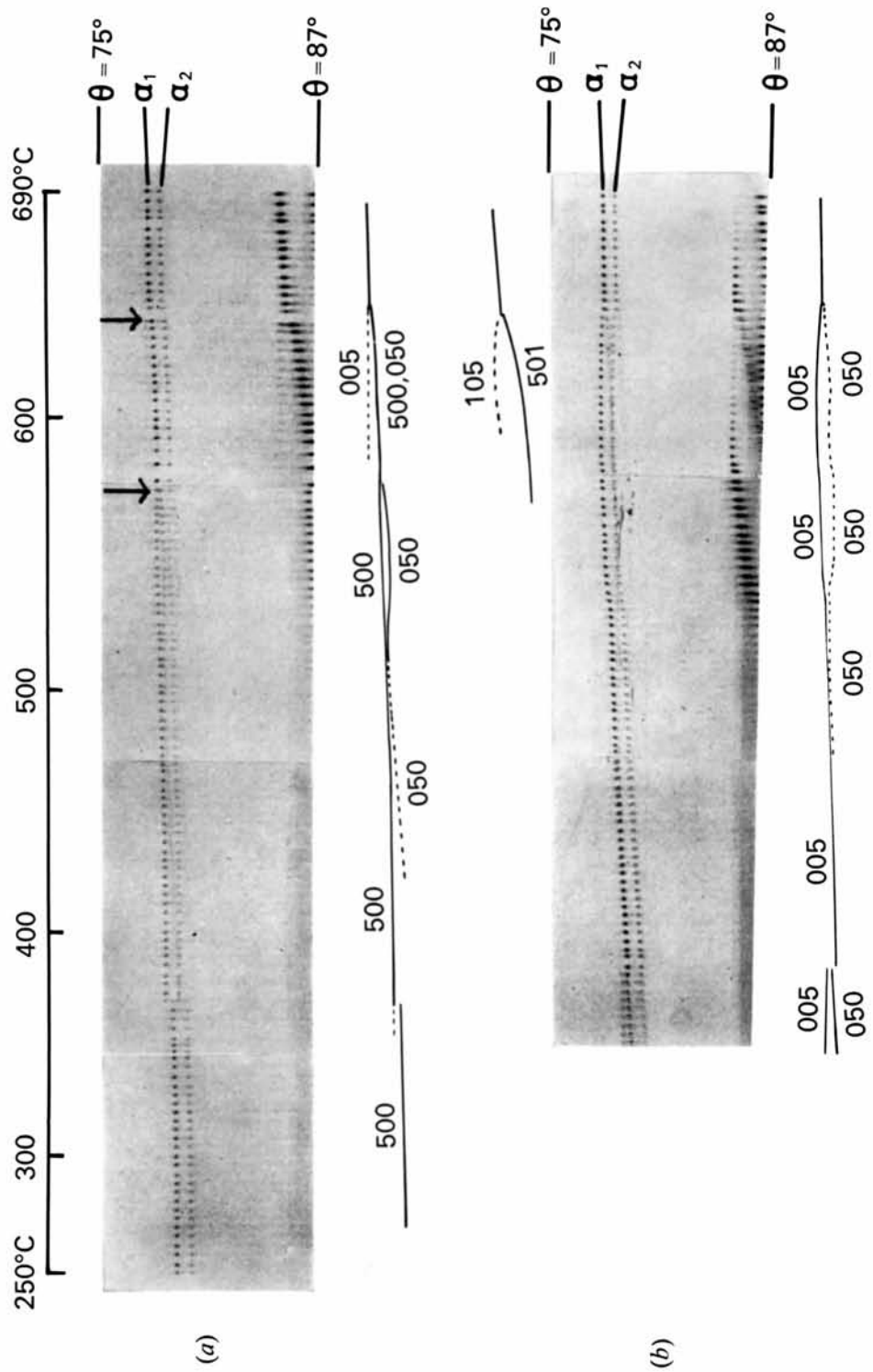

Fig. 3. Back-reflexion oscillation photographs continuously recorded as a function of temeprature. Cu $K\alpha$ radiation. Incremental exposure 5 min. (*a*) Composite of four photographs between $\theta = 75$ and $\theta = 87°$ The temperature was raised at a rate of $\frac{1}{4}$ °C/min. (*b*) Composite of three photographs with the temperature decreasing at a rate of $\frac{1}{4}$ °C/min. Vertical arrows indicate the 575 and 641 °C transitions. The line drawings show the variation in the α_1 components of the reflexions. Note the close similarity with the phase diagram of Fig. 2(*a*).

To face p. 492

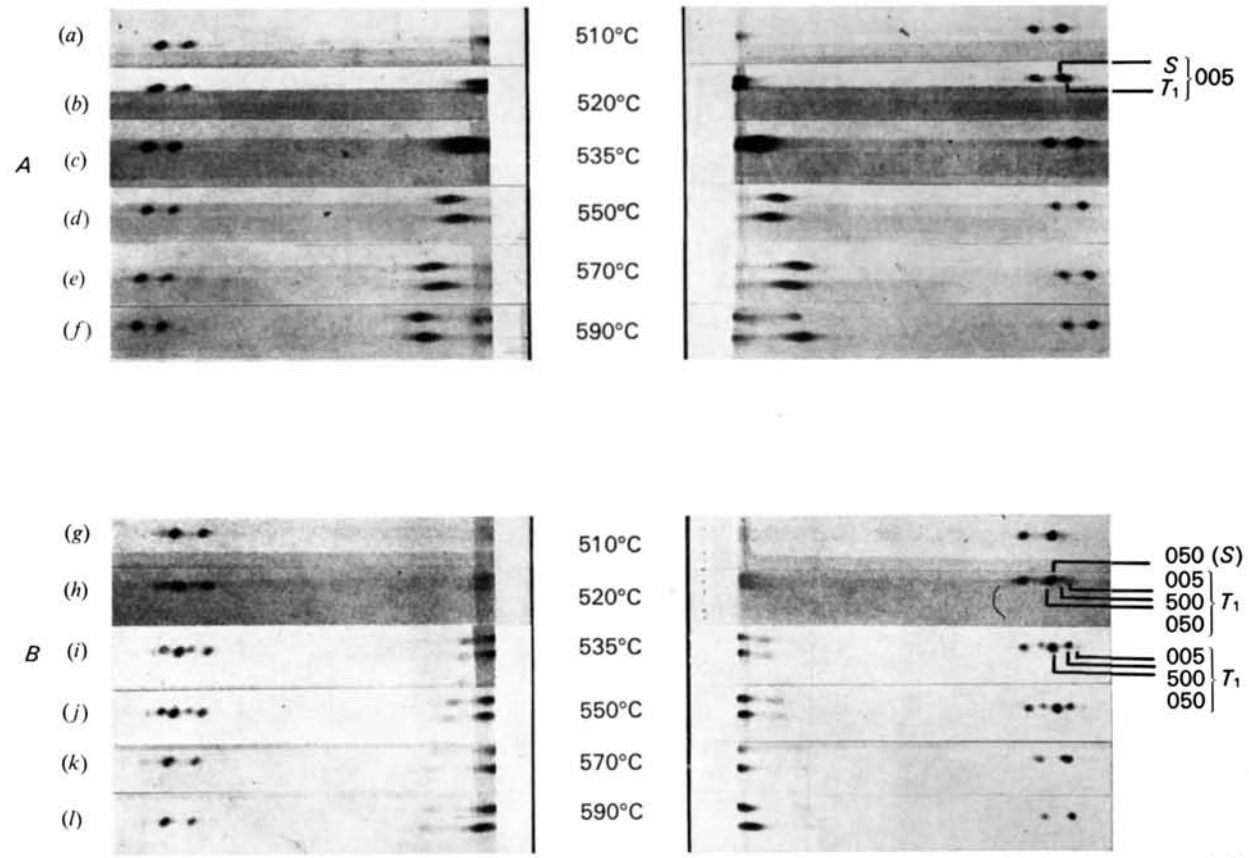

Fig. 5. A series of Cu $K\alpha$ back-reflexion oscillation photographs between 510 and 590°C for two oscillation ranges A and B at 90° to one another, providing information about two of the faces of the crystal. The principal reflexions shown (outer reflexions on the photograph) are the 500 complex (with respect to pseudocubic subcell axes): the inner ones are part of the 510 complex. Azimuth A: (*a*) 005 α_1 and α_2 (phase S); (*b*) 005 α_1 and α_2 (phase S and T_1 together); (*c*) 005 α_1 and α_2 (phase T_1 mainly); (*d*) 005 α_1 and α_2 (phase T_1); (*e*) 005 α_1 and α_2 (phase T_1); (*f*) 005 α_1 and α_2 (phase T_2). Azimuth B; (*g*) 050 α_1 and α_2 (phase S); (*h*) Main spots 050 α_1 and α_2 (phases S and T_1 together), with weak 500 and very weak 005 (due to twinning in T_1); (*i*) Main spots 050 α_1 and α_2 (phase T_1) with weak 500 and very weak 005; (*j*) Same spots; (*k*) 050 α_1 and α_2, phase T_1 (on the r.h.s. of the photograph 050 and 500 are just visible separately; on the l.h.s. they overlap); (*l*) 050 α_1 and α_2 indistinguishable (tetragonal T_2 phase). Differences in background arise from the overlap of successive exposures on the same film, when a wide layer-line screen gap was used, and are not significant.

c_p kept their orientations unchanged. This is done instead of the more usual convention of naming the lattice parameters according to a particular sequence of axial length [for example, the specification $b>a>c$ which is used in *Crystal Data* (Donnay & Donnay, 1963)]. It turns out that at the 373 and 480 °C transitions a sequence $a_p \geq c_p \geq b_p$ is maintained on either side; at the 520 °C transition there is a sharp reversal in the relative lengths of a_p and c_p; and at the 575 °C transition the new sequence, $c_p > a_p \geq b_p$, is maintained.

In order to understand the general rule of continuity of axial directions it is necessary to consider the structures of the various phases, particularly with regard to their arrangements of tilted octahedra. A systematic nomenclature derived earlier by Glazer (1972*b*) is useful in this connexion. In this scheme we consider the tilted arrangements in terms of three component tilts about the three pseudocubic axes. Symbolically, any tilt scheme can be written

$$a^i b^j c^k$$

where the positions of the three symbols refer to the tilts about [100], [010] and [001] respectively, the letters *a*, *b*, *c* denoting their relative magnitudes (so that if two are equal we use the same letter), and the superscripts *i*, *j*, *k* indicating whether successive octahedra along the axis concerned have the same (+), opposite (−), or zero (0) tilts about the axis. For example, $a^-b^+a^-$ has its tilts about [100] and [001] equal in magnitude, and both of them alternate in sense along the respective axes, while the tilt about [010] is of different magnitude and keeps the *same* sense for successive octahedra along this axis. Again, the ideal perovskite structure with no tilts about any axis would have the symbol $a^0a^0a^0$.

With reference to Table 1 the transitions from *R* upwards can be summarized, at least as far as the tilts are concerned, by the scheme

$$a^-b^+c^+;\ a^-b^0c^+ \xrightarrow{480\,^\circ C} a^-b^+c^+ \xrightarrow{520\,^\circ C}$$
$$a^-b^0c^+ \xrightarrow{575\,^\circ C} a^0a^0c^+ \xrightarrow{641\,^\circ C} a^0a^0a^0.$$

We see that throughout the transitions no changes occur in the *senses* of tilt, only in their *magnitudes*.

This empirical observation can be explained as follows. A change in the sense of one tilt, when others are present, would represent a major reorganization of the structure. Assuming the Nb array to remain fixed, one can envisage two processes by which the sense of a tilt could be reversed. In one case, as illustrated in Fig. 4, instantaneous shortening of the Nb–O bond lengths would occur at an intermediate stage; in the other case an instantaneous sharp increase in the magnitudes of tilts about other axes would be operative. Obviously either distortion corresponds to the surmounting of a large energy barrier.

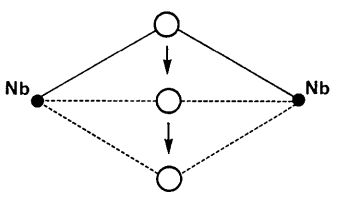

Fig. 4. The effect of changing the sense of tilt in an octahedral layer. During the process the O atom passes between the Nb atoms causing a decrease in NbO bond length at the intermediate stage.

Our rule of continuity of axial directions between phases on either side of a transition is a consequence of the continuity of tilt senses. It is not directly dependent on the axial lengths. The reversal in the relative lengths of a_p and c_p at 520 °C is in fact explained by a reversal in the *magnitudes* of the angles of tilt about [100] and [001], their *senses* remaining unaltered.

When the temperature is changed more rapidly, the simple rule of continuity of tilt senses and axial directions at the transitions is not always followed. Instead, we find twin formation, implying a variety of orientations.

Particular interest attaches to the 520 °C transition. This is illustrated by the series of photographs in Fig. 5. Above the transition we find that the axial reflexions are split into two. This is because of the coexistence of phases *S* and T_1. Fig. 5(*b*) has a strong 005 (inner) component from phase *S* and a weak 005 (outer) component from phase T_1 (not exactly on the same horizontal level). As the temperature increases the phase *S* component weakens and the phase T_1 component strengthens, as seen in Fig. 5(*c*), (*d*). In Fig. 5(*h*) the splitting of 050 due to coexistence of phases *S* and T_1 is more difficult to see, except in so far as it affects the spot shape. This is further complicated by the occurrence of twinning in phase T_1 [particularly clear in Fig. 5(*i*) and (*j*), which no longer show signs of phase *S*]. At both azimuths it is evident in 5(*b*) and 5(*h*), from the relative heights of the component reflexions above a horizontal line drawn through the reflexions, that the *S* phase is concentrated mainly in a domain at one end of the crystal and T_1 at the other (close to the thermocouple junction).

We may suggest an explanation for this coexistence of phases as follows.

In going through the transition, even though the senses of tilt remain unaltered, the abrupt change in their magnitudes implies the existence of a significant energy barrier. With the faster heating rates, conditions within the crystal are likely to be non-uniform and equilibrium cannot be attained instantaneously at the true transition temperature (520 °C). We may suppose that small domains of T_1 appear at this temperature, but that the strains in the T_1–*S* domain walls (a consequence of the difference in lattice parameters) prevent the growth of these T_1 domains and stabilize the continued existence of *S*. As the temperature rises, the changes of lattice parameter cause changes in strain, until at some higher temperature (about 535 °C

in our experiments) the distribution and magnitude of the strains have become critical, and allow growth of T_1 with the consequent disappearance of S. The relief of strain is accompanied by a tendency for twin formation, as in 5(*i*) and 5(*j*). This occurs at azimuth B where the b_p axis is perpendicular to one of the surfaces of the crystal both in phase S and initially in phase T_1. Since the tilt about this axis is zero in T_1, it can easily be interchanged either with the + tilt about a_p or the − tilt about c_p. As a result, on this face, twin domains with any of the three axes perpendicular to the surface can exist.

An indication that this mechanism, or one very much like it, is correct comes from a study of our material by differential thermal analysis (DTA) kindly undertaken by Professor M. Lambert (private communication). In this, reproduced in Fig. 6, two peaks (endothermic with increasing temperature) are observed close to 520 °C. The higher-temperature peak is always broader than the lower one and is dependent on the direction of temperature change; it is broader for cooling than for heating. Neither the peak near 520 °C nor any of the other peaks associated with the other transitions show this anomalous behaviour. On heating, the sharp peak at 520 °C corresponds to the initial formation of T_1 and the broader peak at higher temperature to the disappearance of S accompanied by twin formation. On cooling from phase T_2 the twinning can be more complex, as is usual in transitions from higher to lower symmetry, tending to make the broad DTA peak even broader.

In earlier work (LLM) the possibility was considered that a phase W might exist between 520 and 530 °C. This was characterized by W-shaped reflexions on photographs similar to ours but taken with a camera of 30·00 mm radius and using rather larger crystals and coarser temperature control. Our present techniques give better resolution and show that W- (or M-) shaped spots can be obtained by twinning at the same time as the coexistence of S and T_1 occurs, *i.e.* if Fig. 5(*b*) is superimposed on Fig. 5(*h*) an M-shaped arrangement results. Thus phase W can be explained on the basis of a combination of coexistence between S and T_1 and twinning, both products of a fast heating rate.

5. Summary and conclusions

In this paper, we have shown how single-crystal methods can be used for accurate determination of lattice parameters of materials undergoing complex phase transitions.

Using these methods, we have established definitely that there are five successive transitions above room temperature in $NaNbO_3$. We have found the relations between lattice parameters on either side of each transition and the preferred orientations of the phases formed at the transitions. For the four highest of the transitions we have correlated the effects with the characters

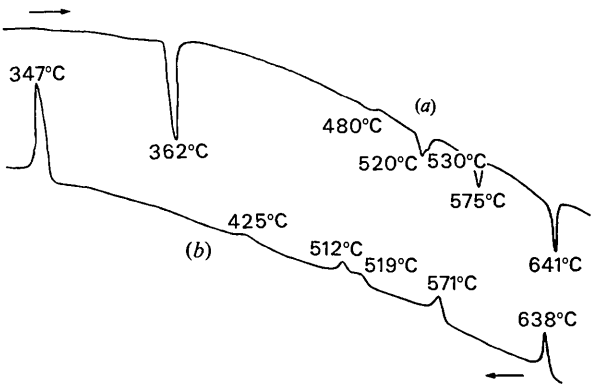

Fig. 6. Differential thermal analysis traces (M. Lambert, private communication) (*a*) with the temperature increasing (endothermic peaks); (*b*) with the temperature decreasing (exothermic peaks). Note the change in shape of the peak at 530 °C [519 °C in (*b*)] and its position relative to the peak at 520 °C [512 °C in (*b*)].

of the octahedral tilts in the different phases. For the 520 °C transition, we have noted the coexistence over a significant temperature range of the two phases concerned.

The fact that we have used very slow and controlled rates of temperature change for our single crystals has made it possible to observe intricate regularities of behaviour that would have been obscured by the inhomogeneous conditions associated with higher rates of change. The use of a double-radius camera has given improved resolution for the interpretation of the X-ray photographs.

We wish to acknowledge our gratitude to the Science Research Council for the support which has made this work possible. We are also grateful to Mr N. Bett and the Electronics Section of the Cavendish Laboratory for help in design and construction of the temperature-controlling system. In addition we should like to thank Professor M. Lambert for carrying out the DTA measurements on our samples.

References

AHTEE, M., GLAZER, A. M. & MEGAW, H. D. (1972). *Phil. Mag.* **26**, 995–1014.

BETT, N. & GLAZER, A. M. (1972). *J. Phys. E: Sci. Instrum.* **5**, 1178–1182.

BUERGER, M. J. (1966). *X-ray Crystallography*, Chap. 20. New York: John Wiley.

COHEN, M. U. (1935). *Rev. Sci. Instrum.* **6**, 68–74.

DARLINGTON, C. N. W. (1971). Ph. D. Thesis, Univ. of Cambridge.

DENOYER, F., COMÈS, R. & LAMBERT, M. (1971). *Acta Cryst.* A**27**, 414–420.

DONNAY, J. D. H. & DONNAY, G. (1963). *Crystal Data.* Part II: *Determinative Tables.* Special monograph No. 5. American Crystallographic Association.

GLAZER, A. M. (1972*a*). *J. Appl. Cryst.* **5**, 420–423.
GLAZER, A. M. (1972*b*). *Acta Cryst.* B**28**, 3384–3392.
GLAZER, A. M. & MEGAW, H. D. (1972). *Phil. Mag.* **25**, 1119–1135.
ISMAILZADE, I. G. (1963). *Kristallografiya*, **8**, 363–367.
LEFKOWITZ, I., ŁUKASZEWICZ, K. & MEGAW, H. D. (1966). *Acta Cryst.* **20**, 670–683.
MILLEDGE, H. J. (1966). *Acta Cryst.* **21**, A220.
SAKOWSKI-COWLEY, A. C. (1967). Ph. D. Thesis, Univ. of Cambridge.
SAKOWSKI-COWLEY, A. C., ŁUKASZEWICZ, K. & MEGAW, H. D. (1969). *Acta Cryst.* B**25**, 851–865.
SOLOV'EV, S. P., VENEVTSEV, YU. N. & ZHDANOV, G. S. (1961). *Kristallografiya*, **6**, 218–224.
TENNERY, V. J. (1965). *J. Amer. Ceram. Soc.* **48**, 537–539.
WOOD, E. A. (1951). *Acta Cryst.* **4**, 353–362.

Acta Cryst. (1973). A**29**, 495

Directions of Dislocation Lines in Crystals of Ammonium Hydrogen Oxalate Hemihydrate Grown from Solution

BY H. KLAPPER* AND H. KÜPPERS

Institut für Kristallographie der Universität Köln, 5 *Köln* 41, *Germany* (*BRD*)

(*Received* 24 *October* 1972; *accepted* 19 *March* 1973)

The defect structures in elastically highly anisotropic crystals of ammonium hydrogen oxalate hemihydrate, $NH_4HC_2O_4.\frac{1}{2}H_2O$, space group *Pnma*, have been studied by X-ray topography. Most of the dislocation lines visible on the topographs are straight and show clearly defined directions which depend on Burgers vector and on growth direction. Burgers vectors parallel to [100], [010], [001], ⟨101⟩ and ⟨011⟩ have been observed. For these Burgers vectors, the variation of energy factor K with direction and the preferential directions of the corresponding dislocation lines in various growth sectors have been calculated. In most cases, observed and calculated directions agree well. The directions of a few dislocations tend to align parallel to low-indexed (symmetry) directions. The influence of the elastic anisotropy on the directions of the dislocation lines as well as the possibility of determining the Burgers vectors from observed preferential directions is discussed.

Introduction

In crystals grown from solution, straight dislocation lines with typical, in general non-crystallographic, directions have been observed (Lang, 1967; Miuskov, Konstantinova & Gusev, 1969; Authier, 1972; Izrael, Petroff, Authier & Malek, 1972; Klapper, 1971, 1972*a*). These preferential directions depend on Burgers vector and on the growth direction of the growth sector concerned. The dependence on growth direction is easily observable when a dislocation penetrates a boundary between different growth sectors: the dislocation line is deflected into a direction which is characteristic of the new growth sector. As previously shown (Klapper, 1971, 1972*a*), those preferential directions may be explained by the following assumption. A dislocation, ending at a growing surface, will proceed into the newly grown layer in such a direction that the elastic energy of the region disturbed by the dislocation within this layer, or, which is the same, the energy per unit growth length, is minimum. Taking into account the elastic anisotropy of the crystals, calculations have been made for dislocations in benzil (Klapper, 1972*b*) and thiourea (Klapper, 1972*b*). Calculated and observed directions agree well.

In this work an investigation of the preferential directions of dislocation lines in crystals of orthorhombic ammonium hydrogen oxalate hemihydrate (AHO), $NH_4HC_2O_4.\frac{1}{2}H_2O$, which exhibit a high elastic anisotropy, is presented. The elastic constants (unit: 10^{11} dyne cm^{-2}) and lattice parameters are (Küppers, 1972*b*, 1973):

$c_{11}=$ 6·71	$c_{12}=$ 1·485	$c_{44}=0{\cdot}383$
$c_{22}=$ 4·14	$c_{13}=$ 0·749	$c_{55}=0{\cdot}592$
$c_{33}=$ 1·48	$c_{23}=$ 1·30	$c_{66}=0{\cdot}973$
$a=11{\cdot}33$	$b=12{\cdot}23$	$c=6{\cdot}90$ Å.

Evidently, the ratio of maximum to minimum longitudinal elastic stiffness is $c_{11}/c_{33}=4{\cdot}5$.

It is the purpose of this study to compare calculated and observed directions and to find out to what extent the observations of preferential directions can be used to determine the Burgers vector. The morphology of the crystals is shown in Fig. 1.

Theory and calculations

The elastic energy W per unit growth length is written (Klapper, 1972*b*):

$$W(\mathbf{e},\mathbf{l},\mathbf{n},c_{ij})=E(\mathbf{e},\mathbf{l},c_{ij})\cos\alpha$$

* Present address: Institut für Kristallographie der Technischen Hochschule Aachen, 51 Aachen, Germany (BRD).